EXPLICIT PSEUDODYNAMIC TEST WITH NUMERICAL DISSIPATION

Shuenn-Yih CHANG[1] And Gee-Yu LIU[2]

SUMMARY

It has been generally recognized that numerical dissipation can effectively suppress the spurious high-frequency responses. The α-function dissipative method developed by the author is a family of second-order dissipative explicit methods. This family of integration methods is very suitable for the pseudodynamic testing since the favorable numerical dissipation can be used to suppress the spurious growth of high-frequency responses due to the presence of numerical and/or experimental errors in performing a pseudodynamic test. Error propagation analysis of this family of integration methods is completed in order to explore the numerical damping effect for the high frequency modes during the pseudodynamic testing. In addition, a simple two degrees of freedom specimen is designed to verify the improved numerical dissipation. The specimen selected is a two degrees of freedom cantilever beam, with the masses chosen to give a high natural frequency and a low natural frequency. For this multiple degree of freedom system, the lower mode is responsible for the seismic response and the higher mode contributes very insignificantly. Both the Newmark explicit method and the α-function dissipative explicit method are employed to perform a series of the pseudodynamic tests.

The error propagation analysis of the α-function dissipative method shows that the suppression of spurious growth of high-frequency response can be obtained and a less error propagation effect is confirmed when compared to the Newmark explicit method. This conclusion is also manifested from the verification test results. Thus, the use of numerical dissipation to eliminate or suppress the high frequency response is benefited in performing a pseudodynamic test.

INTRODUCTION

It is generally recognized that the well control of pseudodynamic errors is the key to yield reliable results since these errors tend to propagate and accumulate from the initiation to the remainder of the test. Pseudodynamic errors introduced in each time step can be reduced if a high performance of test equipment is employed. Besides, it is also very important to select an appropriate integration method to perform the step-by-step integration since a good pseudodynamic algorithm will exhibit a less error propagation effect and thus leads to more accurate test results.

In general, the high-frequency modes of spatially discretized equations of motion do not represent the real behavior of the original structure. In addition, the numerical errors will excite the spurious growth of the high-frequency responses and this effect will be significantly aggravated by the presence of experimental errors in performing a pseudodynamic test. Therefore, it is advantageous for an integration algorithm to have numerical dissipation to suppress or eliminate the high-frequency responses. It has been discovered in the prior studies [Shing and Mahin, 1983, 1984,1987b and 1990] that cumulative errors of a pseudodynamic test are increased with the value of the natural frequency of the test specimen times the step size. This indicates that a more severe error propagation effect will be encountered in the higher modes than in the lower modes. In fact, the spurious growth of high frequency responses may significantly contaminate the test results if the pseudodynamic errors are systematic and of the energy-addition type [Shing and Mahin, 1983]. Thus, a dissipative integration method is generally preferred since it can effectively eliminate this spurious growth of higher modes [Chang, 1997, Shing and Mahin, 1987a] while the lower modes can be integrated very accurately. Recently, the $\alpha-$function dissipative explicit method is successfully developed and shown to possess the desired numerical dissipation

[1] *NCREE, National Taiwan University, Taipei, Taiwan Email: sychang@email.ncree.gov.tw*
[2] *NCREE, National Taiwan University,Taipei, Taiwan Email: karl@email.ncree.gov.tw*

[Chang, 1997]. In order to investigate its performance in pseudodynamic tests, this integration method is carefully implemented and its error propagation effect is also thoroughly analyzed. Finally, a series of verification tests are performed.

A DISSIPATIVE EXPLICIT PSEUDODYNAMIC TEST METHOD

A direct integration method is in general needed in performing a pseudodynamic test [Takanashi *et. al.*, 1975] since its procedure is very similar to the step-by-step time history analysis except that the measured restoring force is used to take place of the mathematical simulation of the restoring force. General expression for the $\alpha-$ function dissipative explicit method can be written as:

$$\begin{aligned} &\mathbf{M}\mathbf{a}_{i+1} + \mathbf{C}\mathbf{v}_{i+1} + (\mathbf{I}+\alpha)\mathbf{r}_{i+1} - \alpha\mathbf{r}_i = \mathbf{f}_{i+1} \\ &\mathbf{d}_{i+1} = \mathbf{d}_i + (\Delta t)\mathbf{v}_i + \frac{1}{2}(\Delta t)^2\mathbf{a}_i \\ &\mathbf{v}_{i+1} = \mathbf{v}_i + \frac{1}{2}(\Delta t)(\mathbf{a}_i + \mathbf{a}_{i+1}) \end{aligned} \tag{1}$$

where $\mathbf{M}$ and $\mathbf{C}$ are the mass and damping matrices; $\mathbf{r}_{i+1}$ and $\mathbf{f}_{i+1}$ denote the restoring force vector and the external force vector. In addition, $\mathbf{d}_{i+1}$, $\mathbf{v}_{i+1}$ and $\mathbf{a}_{i+1}$ represent the vectors of displacements, velocities, and accelerations, respectively. The subscript $i+1$ indicates the time step at $t=(i+1)(\Delta t)$ and $\mathbf{I}$ is used to denote an identity matrix. The restoring force vector $\mathbf{r}_{i+1}$ also can be expressed as $\mathbf{r}_{i+1} = \mathbf{K}\mathbf{d}_{i+1}$ where $\mathbf{K}$ is the tangent stiffness matrix. The matrix coefficient α is defined to be:

$$\alpha = \sum_{i=1}^{\infty} c_i \left[(\Delta t)^2 \mathbf{M}^{-1}\mathbf{K}_0\right]^i \tag{2}$$

where scalar coefficients c_i are appropriate constants. It has been shown that only the first one or two terms are good enough to yield the desired numerical dissipation [Chang, 1997]. It is worth noting that the initial stiffness matrix $\mathbf{K}_0$ is different from the tangent stiffness matrix $\mathbf{K}$. This integration algorithm will become the well-known Newmark explicit method [Newmark, 1959] if $\alpha = 0$.

In this study only the first term on the right hand side of Eq.(2) will be considered. Basic numerical characteristics of the $\alpha-$ function dissipative explicit method have been thoroughly explored in Reference [Chang, 1997] and will not be elaborated here. However, the variation of the numerical dissipation versus the value of $\Omega = \omega(\Delta t)$, where ω is the natural frequency of a linear single-degree-of-freedom system and Δt is size of integration time step, for different values of c_1 is plotted in Fig.(1).

Before performing a pseudodynamic test, it is necessary to determine the initial stiffness matrix $\mathbf{K}_0$ to yield the coefficient matrix α, which will be kept unchanged for the whole test. For each time step, the displacement increment $\mathbf{d}_{i+1} - \mathbf{d}_i$ can be computed from the second equation of Eq.(1), and is quasi-statically imposed upon the specimen by using servo hydraulic actuators. The restoring forces developed by the specimen are measured immediately after the stop movement of actuators and sent back to the computer for the subsequent computations. Next, the velocity and acceleration can be obtained from the first and third equations of Eq.(1). This procedure can be repeated until the desired response time history is achieved.

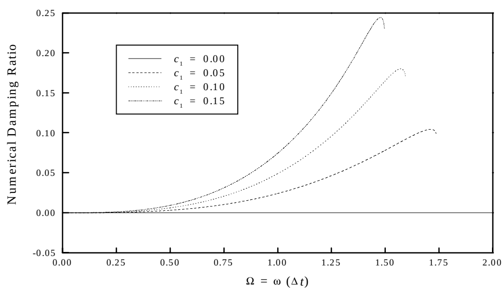

Figure 1: Variation of numerical damping ratio versus Ω

ERROR PROPAGATION ANALYSIS

In performing a pseudodynamic test, it is very difficult to exactly impose the computed displacements upon the test structure due to the displacement control errors and thus results in the incorrect restoring forces [Chang, 1992, Shing and Mahin, 1983]. In addition to the displacement control errors, the actually developed restoring forces may be incorrectly measured and sent back to the computer with errors. Hence, these errors will lead to the force feedback errors and be carried over to the subsequent computations. Obviously, the error propagation effect is that the incorrect imposed displacement leads to the incorrect force feedback and the incorrect restoring force results in the incorrect displacement, which will be imposed upon the specimen for the next step. Consequently, it is very important to evaluate the error propagation effect for a step-by-step integration method since the accuracy of the pseudodynamic test results are closely related to it.

It has been shown that a linear pseudodynamic test will experience more severe error propagation effect when compared to a nonlinear pseudodynamic test and the error propagation properties for a linear multi-degree-of-freedom system can be deduced from the results of a linear single-degree-of-freedom system based on the modal superposition method. Thus, the error propagation analysis is in general performed for a linear single-degree-of-freedom system. The error propagation analysis procedure developed in References [Shing and Mahin, 1983, 1987b] will be employed here. For an undamped single-degree-of-freedom system, the general expression for the $\alpha-$ function dissipative explicit method can be written as:

$$
\begin{aligned}
& m a_{i+1} + (1+\alpha) r_{i+1} - \alpha r_i = f_{i+1} \\
& d_{i+1} = d_i + (\Delta t) v_i + \frac{1}{2} (\Delta t)^2 a_i \\
& v_{i+1} = v_i + \frac{1}{2} (\Delta t)(a_i + a_{i+1})
\end{aligned}
\tag{3}
$$

where α is a scalar and is:

$$
\alpha = \sum_{i=1}^{\infty} c_i \left[(\Delta t)^2 \left(\frac{k}{m} \right) \right]^i \tag{4}
$$

in which m and k are the mass and stiffness of the system, f_{i+1} is the external force; d_{i+1}, v_{i+1} and a_{i+1} are the approximations to the displacement, velocity and acceleration, and r_{i+1} is the measured restoring force.

In performing the error propagation analysis, it will be convenient to introduce the following scalar notations for the subsequent derivations and discussions.

d_i = exact numerically computed displacement at step i without errors.

d_i^e = exact displacement at step i, including the effects of errors at previous steps.

d_i^a = actual displacement at step i, including the effects of previous errors and errors introduced at the current step.

r_i = exact numerically computed restoring force at step i without errors.

r_i^e = exact restoring force at step i, including the effects of errors at previous steps.

r_i^a = actual restoring force at step i, including the effects of previous errors and errors introduced at the current step.

e_i^d = displacement error introduced at step i.

e_i^r = force error introduced at step i.

Based on the above definitions for the displacement and force quantities, it is very straightforward to construct the following equations:

$$\begin{aligned} d_{i+1}^{a} &= d_{i+1}^{e} + e_{i+1}^{d} \\ r_{i+1}^{a} &= r_{i+1}^{e} + e_{i+1}^{r} \end{aligned} \tag{5}$$

In addition, the relationship $e_{i+1}^{r} = ke_{i+1}^{rd}$ is also introduced and thus e_{i+1}^{rd} denotes the amount of displacement error corresponding to e_{i+1}^{r}.

If there does not exist any errors in an idealized pseudodynamic test, the computing procedure for the use of the $\alpha-$function dissipative explicit method can be written in a recursive matrix form as:

$$\mathbf{X}_{i+1} = \mathbf{D}\mathbf{X}_{i} - (1+\alpha)\mathbf{l}r_{i+1} + \alpha\mathbf{l}r_{i} + \mathbf{l}f_{i+1} \tag{6}$$

However, for an actual pseudodynamic test, the displacement and force errors are inevitable. Thus, based on the actual displacements and restoring forces, Eq.(6) becomes:

$$\mathbf{X}_{i+1}^{e} = \mathbf{D}\mathbf{X}_{i}^{a} - (1+\alpha)\mathbf{l}r_{i+1}^{a} + \alpha\mathbf{l}r_{i}^{a} + \mathbf{l}f_{i+1} \tag{7}$$

In the derivations of Eqs.(6) and (7), the following notations are adopted:

$$\mathbf{X}_{i} = \begin{bmatrix} d_{i} \\ (\Delta t)v_{i} \\ (\Delta t)^{2} a_{i} \end{bmatrix} \;,\quad \mathbf{X}_{i}^{e} = \begin{bmatrix} d_{i}^{e} \\ (\Delta t)v_{i}^{e} \\ (\Delta t)^{2} a_{i}^{e} \end{bmatrix} \;,\quad \mathbf{X}_{i}^{a} = \begin{bmatrix} d_{i}^{a} \\ (\Delta t)v_{i}^{a} \\ (\Delta t)^{2} a_{i}^{a} \end{bmatrix} \;,\quad \mathbf{D} = \begin{bmatrix} 1 & 1 & \frac{1}{2} \\ 0 & 1 & \frac{1}{2} \\ 0 & 0 & 0 \end{bmatrix} \;,\quad \mathbf{l} = \frac{(\Delta t)^{2}}{m}\begin{bmatrix} 0 \\ \frac{1}{2} \\ 1 \end{bmatrix} \tag{8}$$

In addition, if r_i and r_i^a are replaced by $\mathbf{S}\mathbf{X}_i$ and $\mathbf{S}\mathbf{X}_i^a$, respectively, where $\mathbf{S} = (k,\ 0,\ 0)$ is introduced, one can have $\mathbf{X}_{i+1} = \mathbf{A}\mathbf{X}_{i} + \mathbf{L}f_{i+1}$ and $\mathbf{X}_{i+1}^{a} = \mathbf{A}\mathbf{X}_{i}^{a} + \mathbf{L}f_{i+1}$ in which the amplification matrix $\mathbf{A}$ and the load vector $\mathbf{L}$ are found to be $\mathbf{A} = [\mathbf{I} + (1+\alpha)\mathbf{l}\mathbf{S}]^{-1}(\mathbf{D} + \alpha\mathbf{l}\mathbf{S})$ and $\mathbf{L} = [\mathbf{I} + (1+\alpha)\mathbf{l}\mathbf{S}]^{-1}\mathbf{l}$, respectively. After defining the cumulative error vector $\varepsilon_{i} = \mathbf{X}_{i}^{e} - \mathbf{X}_{i}$, the following equation can be obtained:

$$\varepsilon_{i+1} = \mathbf{A}\varepsilon_{i} + \mathbf{B}\mathbf{e}_{i}^{d} + \mathbf{C}\left[\alpha\mathbf{e}_{i}^{rd} - (1+\alpha)\mathbf{e}_{i+1}^{rd}\right] \tag{9}$$

where $\mathbf{B} = [\mathbf{I} + (1+\alpha)\mathbf{l}\mathbf{S}]^{-1}\mathbf{D}$ and $\mathbf{C} = [\mathbf{I} + (1+\alpha)\mathbf{l}\mathbf{S}]^{-1}\mathbf{l}\mathbf{S}$. Assuming $\varepsilon_{0} = 0$ and performing a series of repeated substitutions, Eq.(9) reduces to:

$$\varepsilon_{n+1} = \sum_{i=0}^{n} \mathbf{A}^{(n-i)}\mathbf{B}\mathbf{e}_{i}^{d} - \sum_{i=0}^{n} \mathbf{A}^{(n-i)}\mathbf{C}\left[\alpha\mathbf{e}_{i}^{rd} - (1+\alpha)\mathbf{e}_{i+1}^{rd}\right] \tag{10}$$

In addition, by means of the spectral decomposition [Clough and Penzien, 1993], the following cumulative equation can be obtained:

$$e_{n+1}^{d} = \sum_{i=0}^{n} \left\{ E_{i}^{d} \cos\left[(n-i)\overline{\Omega} + \theta\right] \right\} e_{i}^{d} - \sum_{i=0}^{n-1} \left\{ E_{i}^{r} \sin\left[(n-i)\overline{\Omega}\right] \right\} \left[\alpha e_{i}^{rd} - (1+\alpha)e_{i+1}^{rd}\right] \tag{11}$$

where $e_{n+1}^{d} = d_{n+1}^{a} - d_{n+1}$ is the cumulative displacement error. On the right hand side of Eq.(11), the first term is the cumulative errors due to displacement feedback errors and the second term is the cumulative errors due to force feedback errors. The symbols E_i^d and E_i^r are used to represent the error amplification factors for the displacement feedback errors and for the restoring force feedback errors at the $i-th$ step, respectively. Their explicit expressions are found to be:

$$E_i^d = \frac{\left(\sqrt{1-\alpha\Omega^2}\right)^{(n-i)}}{\sqrt{1-\frac{1}{4}(1+\alpha)^2\Omega^2}} \quad , \quad E_i^r = \frac{\left(\sqrt{1-\alpha\Omega^2}\right)^{(n-i)}\Omega}{\sqrt{1-\frac{1}{4}(1+\alpha)^2\Omega^2}} \quad , \quad \theta = \frac{\frac{1}{2}(1+\alpha)\Omega}{\sqrt{1-\frac{1}{4}(1+\alpha)^2\Omega^2}} \tag{12}$$

where θ is a phase angle, n is the total number of time steps and i is the specific $i-th$ time step. It is very interesting to consider the case of $\alpha = 0$ to represent that for the Newmark explicit method:

$$E_i^d = \frac{1}{\sqrt{1-\frac{1}{4}\Omega^2}} \quad , \quad E_i^r = \frac{\Omega}{\sqrt{1-\frac{1}{4}\Omega^2}} \quad , \quad \theta = tan^{-1}\left[\frac{\frac{1}{2}\Omega}{\sqrt{1-\frac{1}{4}\Omega^2}}\right] \tag{13}$$

It is manifested from Eq.(12) that E_i^d and E_i^r depend upon the value of $(n-i)$ while they are independent of $(n-i)$ for the Newmark explicit method as indicated in Eq.(13).

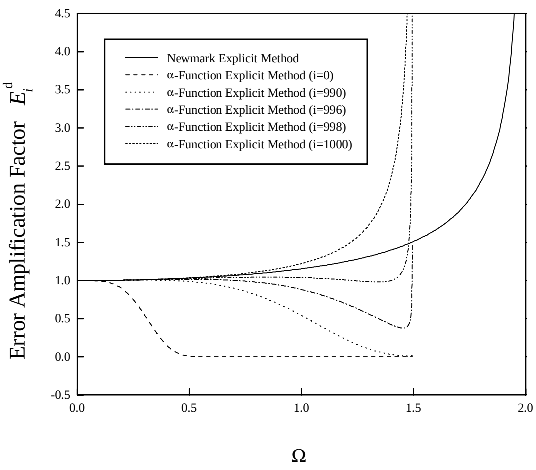

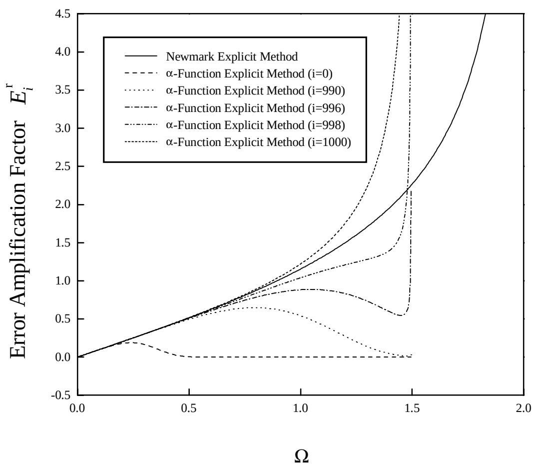

Figure 2: Error amplification factor for displacement Feedback error $(\alpha = 0.15)$

Figure 3: Error amplification factor for restoring force feedback error $(\alpha = 0.15)$

In order to clearly distinguish the error amplification factors between the Newmark explicit method and the $\alpha-$function dissipative explicit method, Eqs.(12) and (13) are further plotted where the total number n is taken to be 1000 time steps and $\alpha = 0.15$ is assumed. Variations of E_i^d versus Ω for the Newmark explicit method and the $\alpha-$function dissipative explicit method are plotted in Fig.(2) and those for E_i^r versus Ω are described in Fig.(3). It is manifested from Fig.(2) that E_i^d for the Newmark explicit method is increased with Ω. This curve moves upward starting from 1 very slowly for small value of Ω while it becomes very rapidly as Ω tends to 2. It is clear that each E_i^d curve for the $\alpha-$function dissipative explicit method is varied with the value of i for a given value of n and it moves upward as the step i increases from 0 to 1000. In addition, it seems that all the E_i^d curves drop from 1 to 0 as Ω increases from 0 to the stability limit for i between 0 and 990. On the other hand, for $990 < i < 1000$, the Newmark explicit method shows larger error amplification factor E_i^d than those of the $\alpha-$function dissipative explicit method and only for $i = 1000$ it shows a smaller value. Thus, the $\alpha-$function dissipative explicit method exhibits less error propagation effect, which is caused by the displacement feedback errors in this figure, when compared to the Newmark explicit method.

Similar phenomena are also found for E_i^r and will not be elaborated here again. The slight discrepancy is that the starting point is 1 for all the E_i^d curves and 0 for all the E_i^r curves. Obviously, this is due to the relation of $E_i^r = \Omega E_i^d$. This error propagation analysis concludes that the $\alpha-$function dissipative explicit method has much better error propagation properties than for the Newmark explicit method. In fact, the $\alpha-$function dissipative explicit method not only possesses less error propagation effect than for the Newmark explicit method but also provide the favorable numerical dissipation in performing a pseudodynamic test.

ACTUAL PSEUDODYNAMIC TESTS

In order to illustrate the favorable numerical dissipation and superior error propagation effect of the $\alpha-$function dissipative explicit method, a series of verification tests are performed in this study.

Test set-up

A cantilever beam is made up of a $3.2m$ long, hot-rolled steel beam and is loaded by 2 static actuators in order to simulate a 2-degrees-of-freedom system. The implementation details are shown in Fig.(4). In the pilot tests, the linear elastic range for the specimen is found to be very small and the built-in LVDT of the actuator can not give an accurate reading of displacement due to the lack of resolution for this small range. The Temposonic III transducer, which is a 24-bit digital sensor, is externally installed along the alignment of each actuator to provide better accuracy in the reading of displacement. These sensors have a feedback signal resolution of $0.005mm$ along the full range of $\pm 250mm$ and were used to take place of the internal LVDT within each actuator.

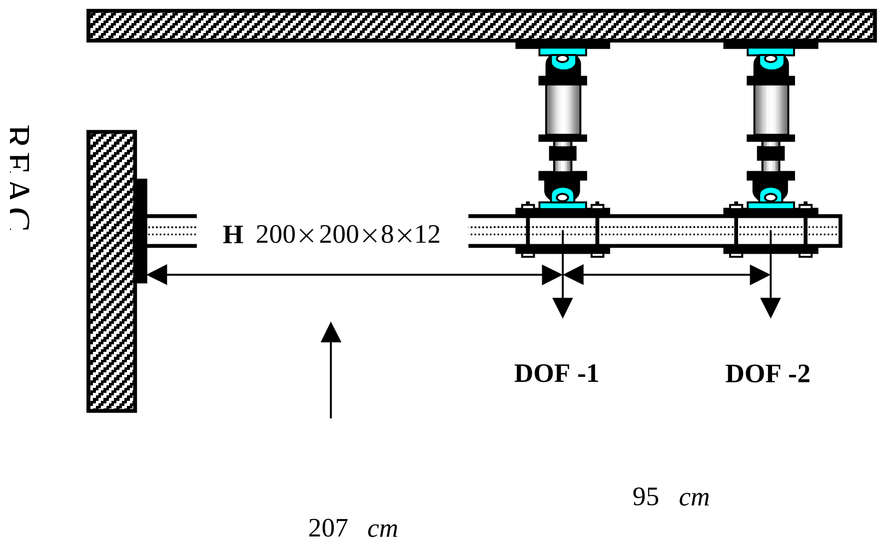

Figure 4: Test set-up for the pseudodynamic testing

Test results

At first, the initial structural stiffness matrix for the test specimen can be experimentally measured and is found to be:

$$\mathbf{K}_0 = \begin{bmatrix} 25.95 & -19.35 \\ -19.35 & 16.35 \end{bmatrix} \tag{14}$$

where the unit for each element is in kN / mm. The lumped masses corresponding to the first and the second degree-of-freedom are specified to be $m_1 = 70535kg$ and $m_2 = 3570kg$. Thus, the natural frequencies of the cantilever beam are $\omega_1 = 6.28 rad / sec$ and $\omega_2 = 70.00 rad / sec$. The structural system is subjected to the El Centro earthquake record with a peak ground acceleration of $0.0025g$. Both the Newmark explicit method and the $\alpha-$function dissipative explicit method with $\alpha = 0.15$ are used to perform the pseudodynamic tests using a time step of $0.02 sec$. All the experimental results from the pseudodynamic tests and the numerical results from analytical simulations are shown in Fig.(5). In computer simulations, 1.6% viscous damping ratio is added into the system to compensate the energy dissipation caused by the friction in the actuator clevis.

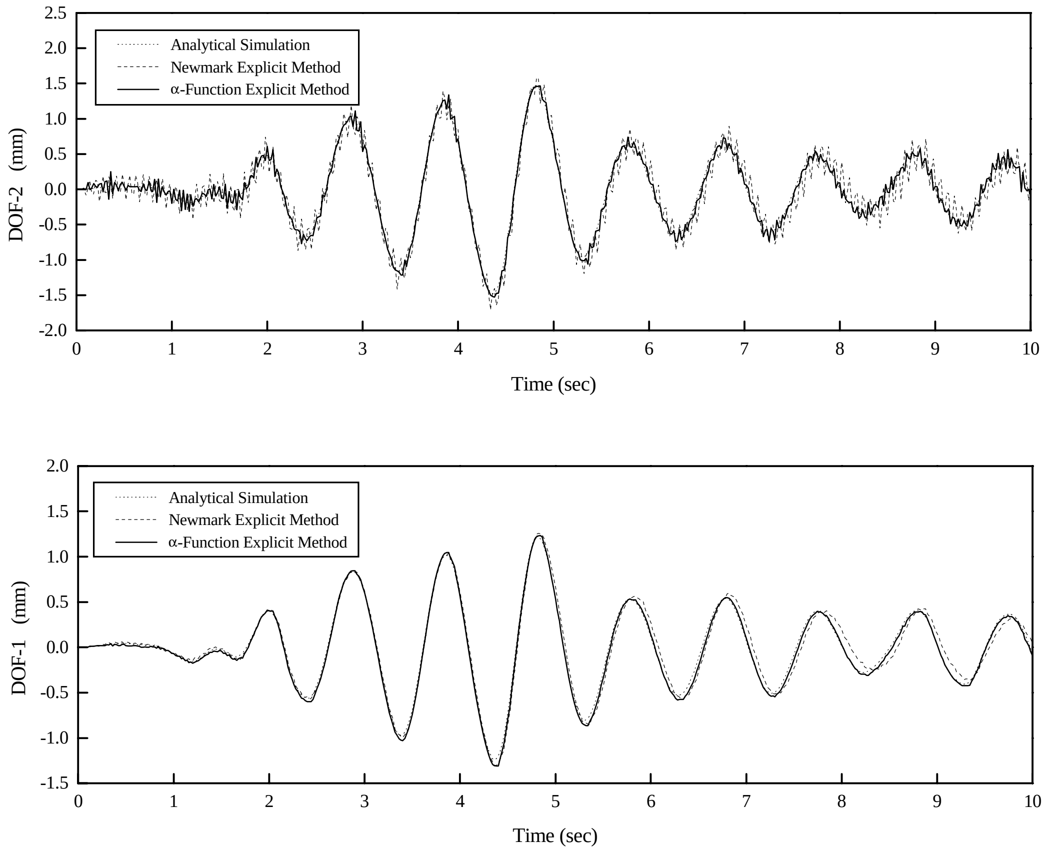

Figure 5: Pseudodynamic response for the 2-DOF system

It is manifested from Fig.(5) that the $\alpha-$function dissipative explicit method with $\alpha = 0.15$ provides more accurate test results than for the use of the Newmark explicit method. Obviously, the cause to different accuracy of the test results between the two integration methods is the numerical dissipation effect and thus the error propagation effect. For the use of $\Delta t = 0.02 sec$, the values of Ω_1 and Ω_2 corresponding to the first and second modes are found to be $\Omega_1 = \omega_1(\Delta t) = 0.126$ and $\Omega_2 = \omega_2(\Delta t) = 1.400$, respectively. Thus, for the $\alpha-$function dissipative explicit method with $\alpha = 0.15$, it will provide about 21.5% numerical damping ratio to suppress the spurious participation of the second mode responses while there is almost no numerical dissipation for the first mode to affect its accurate integration. On the other hand, the Newmark explicit method is a non-dissipative integration method and can not give any numerical dissipation for the two modes. Hence, the errors introduced in the second mode may be more significantly propagated and accumulated than for the $\alpha-$function dissipative explicit method with $\alpha = 0.15$ as indicated in the Figs.(2) and (3) even though the first mode response can be very accurately integrated. As a result, the pseudodynamic test results might be severely contaminated or even entirely destroyed.

CONCLUSIONS

The $\alpha -$function dissipative explicit pseudodynamic algorithm is successfully implemented and tested herein to illustrate its improved numerical dissipation and superior error propagation effect. This explicit integration method exhibits the favorable numerical dissipation since it has a zero damping at the origin and then turns upward gradually. Finally it becomes very steeply as Ω approaches to the stability limit. This strongly indicates that the spurious growth of high frequency responses will be effectively eliminated while the lower modes can be integrated very accurately in performing a pseudodynamic test. In addition to the numerical dissipation effect, this pseudodynamic algorithm also shows much better error propagation effect when compared to the very commonly used Newmark explicit method. Error propagation analysis implies that the elimination or suppression of the spurious growth of the high frequency responses will also lead to the less error propagation effect than for a non-dissipative pseudodynamic algorithm. Consequently, the $\alpha -$function dissipative pseudodynamic algorithm is very suitable for the test structure with high frequency modes and the high frequency responses are of no interest.

ACKNOWLEDGMENTS

The author is grateful to acknowledge that this study was financially supported by the National Science Council, Taipei, Taiwan, R.O.C., under Grant No. NSC-88-2711-3-319-200-20.

REFERENCES

Chang, S.Y. (1992), “Two New Implicit Algorithms of Pseudodynamic Test Methods,” Thesis for Master of Engineering, University of California, Berkeley.

Chang, S.Y. (1997), “Improved Numerical Dissipation for Explicit Methods in Pseudodynamic Tests,” *Earthquake Engineering and Structural Dynamics*, 26, pp917-929.

Clough, R.W. and Penzien, J. (1993), *Dynamics of Structures*, McGraw-Hill, New York.

Newmark, N.M. (1959), “A Method of Computation for Structural Dynamics,” *Journal of the Engineering Mechanics Division*, ASCE, pp67-94.

Shing, P.B. and Mahin, S. A. (1983), *Experimental Error Propagation in Pseudodynamic Testing*, UCB/EERC-83/12, Earthquake Engineering Research Center, University of California, Berkeley, CA.

Shing, P. B. and Mahin, S. A. (1984), *Pseudodynamic Method for Seismic Performance Testing: Theory and Implementation*, UCB/EERC-84/01, Earthquake Engineering Research Center, University of California, Berkeley, CA.

Shing, P.B. and Mahin, S. A. (1987a), “Elimination of spurious higher-mode response in pseudodynamic tests,” *Earthquake Engineering and Structural Dynamics*, 15, pp425-445.

Shing, P.B. and Mahin, S. A. (1987b), “Cumulative experimental errors in pseudodynamic tests,” *Earthquake Engineering and Structural Dynamics*, 15, pp409-424.

Shing, P.B. and Mahin, S. A. (1990), “Experimental error effects in pseudodynamic testing,” *Journal of Engineering Mechanics, ASCE* 116, pp805-821.

Takanashi, K., Udagawa, K., Seki, M., Okada, T. and Tanaka, H. (1975), *Nonlinear Earthquake Response Analysis of Structures by a Computer-Actuator On-line System*, Bulletin of Earthquake Resistant Structure Research Center, 8, Institute of Industrial Science, University of Tokyo, Tokyo, Japan.